# Printed leaky-wave antenna with aperture control using width-modulated microstrip lines and TM surface-wave feeding by SIW technology

# Printed Leaky-Wave Antenna with Aperture Control using Width-Modulated Microstrip Lines and TM Surface-Wave Feeding by SIW Technology

Maksim V. Kuznetcov, *Student Member, IEEE*, Victoria Gómez-Guillamón Buendía, *Student Member, IEEE*, Zain Shafiq, *Student Member, IEEE*, Ladislau Matekovits, *Senior Member, IEEE*, Dimitris E. Anagnostou, *Senior Member, IEEE*, Symon K. Podilchak, *Member, IEEE*

***Abstract*—The article presents a width-modulated microstrip line leaky-wave antenna (LWA) with substrate integrated waveguide and microstrip feeding. In particular, the planar antenna system consists of an integrated surface-wave launcher and three identical rows of quasi-periodic width-modulated microstrip lines for TM leaky-wave excitation which produces a tailored binomial-like aperture distribution on the guiding surface. The behavior of the antenna when changing the width-modulated lines for different aperture distributions is also analysed and presented. The measured LWA demonstrates a fan beam pattern in the far-field with realized gain values greater than 10 dBi and with a beam direction of about -20° from broadside at 23 GHz. Also, far-field measurements and near-field data indicate that the half-power beamwidth is below 10° and the position of the main beam maximum is relatively stable; i.e. ranging from about -23° to -15° between 23 to 24 GHz. The measured prototype is also well matched over these frequencies and $|S_{11}| <$ -20 dB at 23.5 GHz.**

## I. Introduction

In modern radio frequency technology, the use of directive beam pattern antennas has different sensor and communication applications such as radar and satellite connectivity. In these systems it is often necessary to have controlled-beam antennas to improve the overall performance of the transceiver system. One solution can be to use leaky-wave antennas (LWAs) and surface-wave (SW) driven structures. Examples include microstrip-based planar antennas [1]–[6], substrate integrated waveguide (SIW) antennas [7], [8], or even hybrid types where planar and metallic technologies are combined [9]–[11]. In general, these antennas can also be used in a wide range of applications for machine-to-machine (M2M) systems [12], charging stations [13], or local Internet of Things (IoT) [14] services. Another application for LWAs is in automotive radar [15]–[17].

One important challenge when designing LWAs is to ensure efficient radiation. To achieve high values, appropriate leaky-wave (LW) field distributions should be synthesized. One possible solution is the use of a sinusoidally-modulated reactive surface (SMRS) [18], [19]. Those LWA designs are based on a printed array of unit cells which consist of metallic strip configurations having different gap-sizes, and by varying the surface reactance as well as the modulation factor and the periodicity, it is feasible to control the LW phase constant $(\beta)$ and the leakage attenuation rate $(\alpha)$. Another approach to achieve a tailored aperture distribution is by holographic principles [20], where radiation can be controlled by altering the unit-cell dimensions. Expanding on these methodologies the antenna engineer can synthesize any desired aperture distribution for LW radiation. Another solution, introduced in the literature, is the use of width modulated microstrip lines within the unit cell [21]–[23]. In contrast with the SMRS from [18] where the fundamental mode (harmonic) radiates, in width-modulated microstrip LWAs, the $n = -1$ spatial harmonic is employed for Bragg radiation [21]–[24].

Following these developments, planar LWAs using Cartesian [21] and Polar [22] aperture arrangements and $TM_0$ surface-wave launchers (SWLs) have been reported [2], [25]. Typically the Yagi-Uda-like SWL uses slots which are integrated within the ground plane of a grounded dielectric slab (GDS) and where the main driven slot is connected to a 50-Ω coplanar transmission line for antenna feeding. A new type of SIW-SWL is developed in this work using a continuous ground plane and no slots for $TM_0$ SW excitation and with a 50-Ω microstrip feed (see Fig. 1). This significantly expands the possible applications for the proposed antenna and simplifies mounting requirements. For example, any antenna which employs the developed SIW-SWL feed system could be easily placed on a car or metallic airplane fuselage.

Also following the earlier work in [21] and [22], a novel width-modulated aperture was reported in [23] that maintained the same LW phase propagation constant over the aperture while also changing $\alpha$; i.e. effectively controlling the leakage while maintaining the same beam angle in the far-field. In these preliminary findings, the control of the unit cell parameters; i.e. the width $W$ and periodicity $D_u$ provided high flexibility for the printed design and can also be utilized to achieve different beam patterns as desired, possibly obtaining high efficiency and low side lobes. Having such a quasi-independent control of $\alpha$ and $\beta$, one can properly cascade the unit cells allowing for a local tailoring of the desired leakage rate along the antenna aperture. To the best of the authors' knowledge a design approach with such flexibility has not yet

Manuscript received Feb. 27th, 2019, resubmitted July 3rd, accepted July 21st. This project has received funding from the European Union's Horizon 2020 research and innovation programme under the Marie Sklodowska-Curie grant agreement 709372 and 840854.

M.V. Kuznetcov, V.G Buendia, Z. Shafiq, D.E. Anagnostou, and S.K. Podilchak are with Heriot-Watt University and The University of Edinburgh, Scotland UK (e-mail: s.podilchak@ed.ac.uk).

L. Matekovits is with Politecnico di Torino, Dipartimento di Elettronica, Italy. (e-mail: ladislau.matekovits@polito.it)

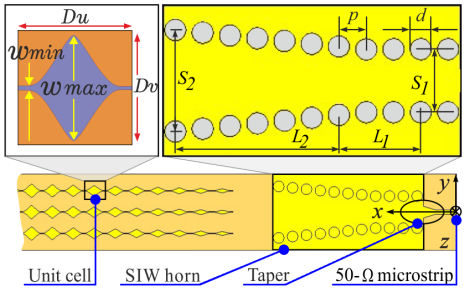


Fig. 1. Proposed 1-D LWA with microstrip feeding and SIW horn antenna for $TM_0$ SW excitation. Dimensions are further defined in Fig. 2(a).

been experimentally verified.

Given these findings, we propose a new LWA. The presented aperture consists of three rows of cascaded unit cells. Within each row, different width-modulated microstrip line geometries are cascaded (see Figs. 1 and 2 (a)) to realize a binomial-like aperture distribution. This has the design motivation to increase radiation efficiency and decrease side-lobe levels whilst employing low-cost printed circuit board technology. Analysis of other types of comparable aperture distributions and their resulting radiation performances are also investigated. Moreover, the proposed binomial-like distribution is simulated and measurement results are close to those of the fabricated prototype. As mentioned, a new type of SIW-SWL is also presented and the design methodology is explained. Measurements and simulations are also presented while taking into account possible manufacturing errors, variation in the dielectric, and minor antenna performance degradation due to the connector. Also, radiation patterns using near-field (NF) and far-field (FF) measurement systems are presented and well compared with these simulations.

## II. Design Procedure

The proposed planar LWA mainly consists of two parts: (1) the width-modulated microstrip unit cells arranged in lines and (2) the SIW horn SWL (see Figs. 1 and 2). The main idea is to excite $TM_0$ SWs from the aperture of the SIW horn antenna which are perturbed by the width-modulated unit cells aiming to obtain controlled LW radiation.

The considered aperture distribution is a binomial-like one with different unit cells generating a beam with low side-lobes. On that basis, and in a similar manner to LWAs with periodic holes or strips [26], [27], the control of $\alpha$ dictates the beam pattern features, such as the beam width, the realized gain, and the side lobe levels. For our proposed LWA we will consider an aperture where $\alpha$ is low at the beginning and at the end, while being high in the middle of the structure (see Fig. 2).

### A. SIW Feed Design for TM SW Generation

Classically SIW horn antennas are of interest due to their low-cost and simple fabrication. For the proposed SIW-SWL it is important to properly choose the dielectric material and thickness since the overall response at microwave and millimeter-wave frequencies can affect the SW excitation efficiency. Thus, our choice of the dielectric substrate was Rogers RT6010 ($\varepsilon_r$ = 10.2, $h$ = 1.27 mm) as it can ensure suitable TM SW launching [2], [25] at the design frequency.

The SWs will be generated at the output of the horn and will propagate along the air-dielectric interface by the dominant mode of the slab; i.e. the $TM_0$ SW mode [28]. This is because the $E_z$ component of the $TE_{10}$-like mode of the SIW horn is field matched to that of the $TM_0$ SW mode of the employed GDS. Also, to improve impedance matching, the flare in the $H_{(x-y)}$ plane of the TM SW horn was optimized using CST to minimize reflections such that $|S_{11}| < -20$ dB.

The final part of SIW feed includes a connecting 50-Ω microstrip line. A taper was included to match the impedances of the microstrip line and the SIW horn. Also, the microstrip line supports a quasi-TEM mode and the SIW line supports a $TE_{10}$ mode [29], of which have similar field configurations. Further details on SIW tapers can be found in [29] and [30].

### B. Aperture Design by Width-Modulated Microstrip

The next part of the antenna structure is the radiating aperture. It consists of a combination of unit cells based on printed microstrip lines with maximum and minimum width values $W_{max}$ and $W_{min}$ (see Fig. 1). Based on holographic antenna principles, the behavior and shape of each unit cell allows the designer to control $\alpha$ and $\beta$. The structure is characterized by the periodicity $D_u$ and $D_v$ in the longitudinal and transverse directions, respectively. For the considered geometry, the frequency behavior of the single unit cell was modeled analytically and follows Mathieu's and Hill's functions [31], [32] as applied in [22]. Also by following [21]–[23], a minimum width of $W_{min}$ = 0.1 mm was selected. Therefore, $D_u$ was varied to change $\beta$, while $D_v$ was kept constant to minimize possible coupling between the transverse unit cells and $W_{max}$ was varied to control $\alpha$ [33] since the modulation index is related to $W_{max}$ of the unit-cell [22].

By selecting the appropriate unit cells the LW field excitation can be controlled in the $x$-direction along the length of the antenna [33]. Figure 2(b) plots the LW phase and attenuation constants given the unit cell dimensions from Fig. 2(a). Also, by having the same pointing angle for each unit cell; i.e. $\hat{\beta}$ = -0.292, (where $\hat{}$ refers to a normalization with respect to $k_0$), it is possible to achieve control of the aperture field. In the present proof of concept LWA, as illustrated in Fig. 1, three identical lines (see Fig. 2) have been considered to generate a fan beam pattern in the FF. Each unit cell as defined in Fig. 2 can be represented as an independent radiation element.

Simulations with a larger aperture show that by using only lines with relatively low and a constant leakage rate $\hat{\alpha} = 0.03$ for comparison (20 unit cells by 9 rows $W_{max}$ = 0.7 mm and $D_u$ = 3.97 mm giving $\hat{\alpha}$ = 0.03) a narrow beam width and higher level of side lobes can be observed when compared to an equivalent structure using the designed binomial-like aperture (see Fig. 3). On the other hand, an aperture with a constant but higher leakage rate ($W_{max}$ = 1.5 mm, $D_u$ = 4 mm, $\hat{\alpha}$ = 0.05) generated a wider beam but with lower side lobe levels. Also, as expected, no distinct side lobes can be observed for the binomial-like aperture and when compared to the apertures defined by a constant leakage rate.

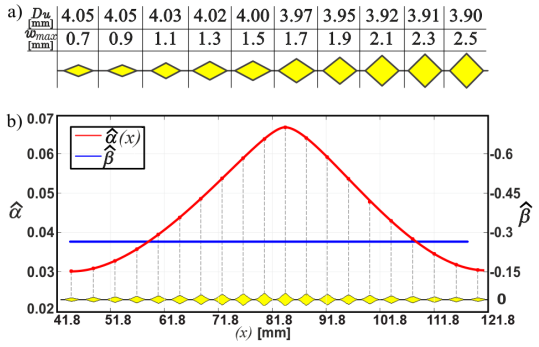


Fig. 2. (a): Dimensions of the width-modulated unit cells for the first half of the aperture. (b): Normalized $\alpha$ and $\beta$ versus length for the 20-element binomial like aperture at 23.5 GHz using the unit cells described in (a). With this geometry $\hat{\alpha}$ is tailored (which changes over the aperture) while the LW propagation constant remains consistent; i.e. $\hat{\beta}$ = -0.292.

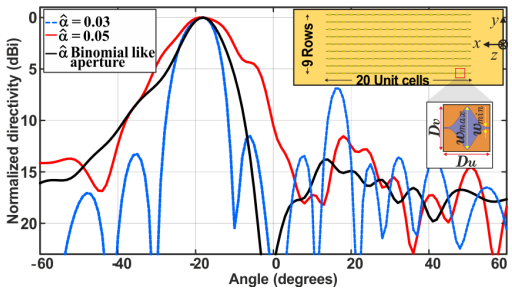


Fig. 3. Normalized directivity for different aperture distributions considering 180 unit-cells at 23.5 GHz for a constant LW aperture with $\hat{\alpha}$ = 0.03 and 0.05. Results are also compared to the arrangement in Fig. 2 and with the same number of unit-cells for the realization of a binomial-like aperture. The designed pointing angle for all the structures is -17° at 23.5 GHz.

It should be mentioned that the LW attenuation constants were computed by simulating each unit cell independently using an aperture with a large number of unit cells representing an almost infinite structure (180 unit cells) as illustrated in Fig. 3 (see inset). This aperture was illuminated with a uniform $TM_0$ SW field distribution originating from the edge of the guiding surface. Then by observing the 3dB beamwidth and pointing angle ($\theta_p = \sin^{-1}\hat{\beta}$) for the radiated beam pattern in the FF, $\hat{\beta}$ could be determined as well as $\hat{\alpha}$ using $BW_{3\text{dB}} = 2\hat{\alpha}\csc\theta_p$ [34]. This procedure allowed us to acquire the relationship between the parameters of the unit-cells and the generated LW field. Mainly, by changing $W_{max}$ and $D_u$ whilst considering a 23.5 GHz design frequency, we were able to construct a design table. Based on this parametric study we were able to synthesize $\alpha(x)$ for a constant $\beta$.

The total radiation efficiency for the different distributions investigated (from Fig. 3) were computed in a commercial full wave simulator CST by taking into account conductor and substrate losses while also considering a consistent aperture (20 unit cells by 9 rows). The predicted beam maximum of the examined structures is -17° at 23.5 GHz (see Fig. 3). As observed, results in Fig. 4 show that the binomial like distribution provides the highest efficiency for all considered apertures with values above 85%.

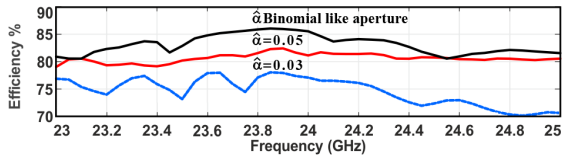


Fig. 4. Simulated radiation efficiency for the LWAs as considered in Fig. 3.


Fig. 5. Fabricated LWA using Rogers RT6010 with a rated relative dielectric constant $\varepsilon_r$ = 10.2, thickness $h$ = 1.27 mm: (a) top view (b) bottom view.

## III. Simulations, Measurements & Discussion

The proposed LWA was designed, simulated and manufactured. A photograph of the prototype is shown in Fig. 5. As described in Table I, previous LWAs operated well below 20 GHz and do not offer any controlled aperture distribution.

In our work, the pitch and diameter of the vias was $p$ = 2.6 mm and $d$ = 2 mm, the distance between one end of vias to another was $S_1$ = 6 mm and $S_2$ = 9.5 mm, while lengths for the SIW horn were $L_1$ = 7.8 mm and $L_2$ = 18.2 mm. Moreover, $W_{min}$ = 0.1 mm (see Fig 1). Dimensions of the structure, i.e. width $W_{max}$ and periodicity $D_u$ of the different modulated unit cells are tabulated in Fig. 2(a). To verify performance in the NF and the FF, the NSI-5912 Near-Field Scanner and the DAMS 7100 Diamond Engineering Far-field Measurement System were used, respectively. Measurements and simulations are compared in Figs. 6-9.

Simulations showed that at the design frequency of 23.5 GHz, the realized gain is 14.2 dBi with a pointing angle of $\theta_p$ = -19°. The beam pattern and the pointing angle of the main beam in the FF over a wide frequency range around 23.5 GHz has been experimentally validated and presented in Figs. 7 and 8 demonstrating LWA operation.

The antenna is well matched for the frequency range 22 to 24 GHz with $|S_{11}|$ values below -10 dB and about -20 dB at the design frequency of 23.5 GHz (see Fig. 9). The employed Southwest end launch SuperSMA (292-04Z-6) type connector was also taken into consideration during simulations, which generated a minor gain drop over frequency and contributed to an angle shift in the main beam position due to electromagnetic coupling between the connector itself and the radiating LW fields. The maximum gain of the antenna with the connector was observed to be 13.4 dBi at 23.2 GHz.

Simulations and measurements shown in Figs. 7, 8, and 9 further take into account all losses and practical variations in the dielectric constant [35]. For the measured structure the maximum realized gain occurs at 23.45 GHz with values of 10.7 dBi as shown in Fig. 8. The reduction in gain is likely related to the connector and a practical change in $\varepsilon_r$ from its rated value. More specifically, simulations showed that practical variations in the relative dielectric constant from 10.2 to 10.6 caused the gain to drop by about 2 dB (see Fig. 8) and

TABLE I
COMPARISON TO SIMILAR LWAS FOUND IN THE LITERATURE

| Reference | Center Frequency | Beam Angle Range | Realized Gain Max | Aperture Control | Side Lobe Level | Efficiency | Radiating Harmonic |
|---|---|---|---|---|---|---|---|
| [19] | 10 GHz | -25° to -35° | 16.6 dBi | Yes | -14.33 dB | - | n = 0 |
| [20] | 15 GHz | 22° to 60° | 17.8 dBi | No | <-10 dB | >95% | n = -1 |
| [24] | 14 GHz | -58° to 35° | 21.3 dBi | No | <-10 dB | 88% | n = -1 |
| This work | 23.5 GHz | -25° to -16° | 14.9 dBi | Yes | <-10 dB | >85% | n = -1 |

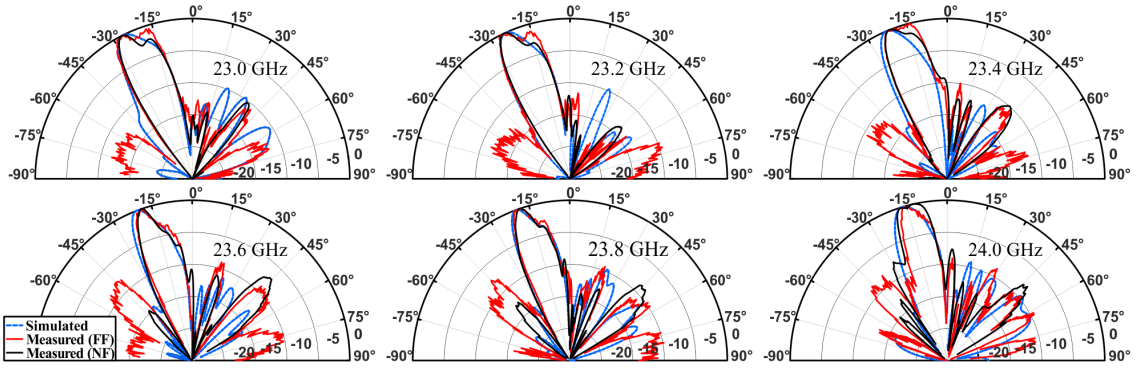


Fig. 6. Measured and simulated radiation patterns for different frequencies from 23 GHz to 24 GHz in the $x$-$z$ plane, demonstrating beam scanning from -25° to -15°. It should be mentioned that the simulations consider a relative dielectric constant of 10.6 and connector for consistency with Figs. 7-9.

the pointing angle at the design frequency is -20° and slightly shifted by about 2° at other frequencies (see Fig. 6).

The minor discrepancy between the simulations and measurements can also be related to manufacturing tolerances e.g. drilling and metalization of the vias. Despite these practicalities, the measurement results are in good agreement with simulations, showing the expected performance, and demonstrating proof of concept. The beam patterns are also plotted in Fig. 7 using both NF and FF measurement approaches and results are in agreement. Also, the measured cross-polarization levels are 10 dB below from the main co-polarized maximum.

It should also be mentioned that the measured LWA has a somewhat narrow operating bandwidth from about 23 GHz to 24 GHz. This is due to the employed design approach where a specific center frequency for radiation was chosen and the unit cells were selected to achieve the required aperture distribution. This is also related to the relatively high dielectric constant ($\varepsilon_r \approx 10$) for the employed GDS to ensure good coupling efficiencies into the dominant $TM_0$ SW mode. These design constraints can be alleviated in future work, for example, by considering a lower dielectric constant for the GDS and with an increased thickness. Mainly because the $TM_0$ SW mode can be less dispersive when using a lower dielectric constant (for example, $\varepsilon_r \approx 2$). This however would require the redesign of the SIW-SWL and aperture distribution. Such an approach would present similar limitations in the beam scanning angle range. In our work we have adopted a LWA structure that exhibits a good compromise between these two main constraints; i.e. good SW coupling efficiency [2], [25] whilst respecting the dispersion of the $TM_0$ SW mode.

## IV. CONCLUSION

We introduced a new type of planar LWA with a new SWL and with 50-Ω microstrip feeding. The proposed SIW-SWL can be used in other types of LWAs where TM SW excitation

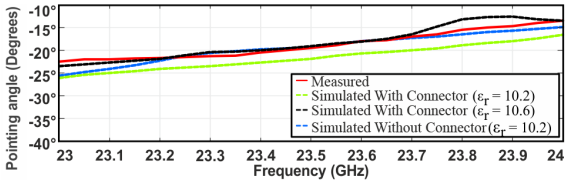


Fig. 7. Beam pointing angle for the proposed LWA (see Fig. 5). A comparison is also provided with and without the connector and $\varepsilon_r$ = 10.2 and 10.6. Note: Figs. 8 and 9 have the same legend as this figure.

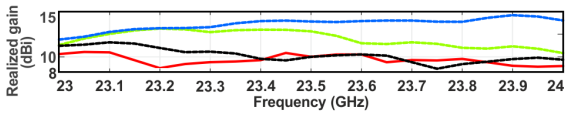


Fig. 8. Measured and simulated maximum realized gain in the $x$-$z$ plane.

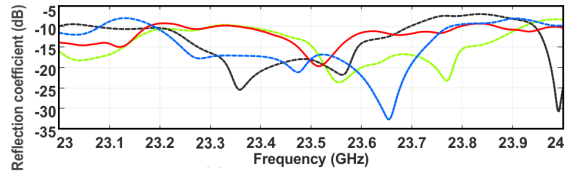


Fig. 9. $|S_{11}|$ for the proposed planar LWA prototype.

is required while also allowing for good efficiency and low-cost implementation. The developed binomial-like distribution represents an alternative to existing approaches found in the literature. The maximum measured realized gain was 10.7 dBi at 23.45 GHz with the main beam direction at about -20°. The experimental radiation patterns are presented and compared with simulations where changes in the dielectric constant and the employed connector were taken into account. The proposed LWA can be used in communication applications such as radar systems where the advantage of having a continuous ground plane allows for placement on cars or airplane fuselages.

## REFERENCES


[1] C. A. Balanis, *Antenna theory: analysis and design*. Wiley-Interscience, 2016.

[2] S. K. Podilchak, P. Baccarelli, P. Burghignoli, A. P. Freundorfer, and Y. M. M. Antar, "Analysis and Design of Annular Microstrip-Based Planar Periodic Leaky-Wave Antennas," *IEEE Transactions on Antennas and Propagation*, vol. 62, no. 6, pp. 2978–2991, June 2014.

[3] P. Baccarelli, P. Burghignoli, G. Lovat, and S. Paulotto, "A novel printed leaky-wave 'bull-eye' antenna with suppressed surface-wave excitation," in *IEEE Antennas and Propagation Society Symposium, 2004.*, vol. 1, June 2004, pp. 1078–1081 Vol.1.

[4] P. F. Kou and Y. J. Cheng, "Ka-band low-sidelobe-level slot array leaky-wave antenna based on substrate integrated nonradiative dielectric waveguide," *IEEE Antennas and Wireless Propagation Letters*, vol. 16, pp. 3075–3078, 2017.

[5] Y. Hou, Y. Li, Z. Zhang, and Z. Feng, "Narrow-width periodic leaky-wave antenna array for endfire radiation based on hansenwoodyard condition," *IEEE Transactions on Antennas and Propagation*, vol. 66, no. 11, pp. 6393–6396, Nov 2018.

[6] Y. Hou, Y. Li, Z. Zhang, and M. F. Iskander, "Microstrip-fed surface-wave antenna for endfire radiation," *IEEE Transactions on Antennas and Propagation*, vol. 67, no. 1, pp. 580–584, Jan 2019.

[7] A. J. Martinez-Ros, J. L. Gomez-Tornero, and G. Goussetis, "Planar Leaky-Wave Antenna With Flexible Control of the Complex Propagation Constant," *IEEE Transactions on Antennas and Propagation*, vol. 60, no. 3, pp. 1625–1630, March 2012.

[8] M. T. Mu and Y. J. Cheng, "Low-sidelobe-level short leaky-wave antenna based on single-layer pcb-based substrate-integrated image guide," *IEEE Antennas and Wireless Propagation Letters*, vol. 17, no. 8, pp. 1519–1523, Aug 2018.

[9] J. L. Gomez-Tornero, G. Goussetis, A. P. Feresidis, and A. A. Melcn, "Control of Leaky-Mode Propagation and Radiation Properties in Hybrid Dielectric-Waveguide Printed-Circuit Technology: Experimental Results," *IEEE Transactions on Antennas and Propagation*, vol. 54, no. 11, pp. 3383–3390, Nov 2006.

[10] U. Beaskoetxea, V. Pacheco-Peña, B. Orazbayev, T. Akalin, S. Maci, M. Navarro-Cia, and M. Beruete, "77-ghz high-gain bull's-eye antenna with sinusoidal profile," *IEEE Antennas and Wireless Propagation Letters*, vol. 14, pp. 205–208, 2 2015.

[11] Y. Hou, Y. Li, Z. Zhang, and M. F. Iskander, "All-metal endfire antenna with high gain and stable radiation pattern for the platform-embedded application," *IEEE Transactions on Antennas and Propagation*, vol. 67, no. 2, pp. 730–737, Feb 2019.

[12] Y. Yang, H. Ye, S. Fei, Y. Yang, H. Ye, and S. Fei, "Design of communication interface for M2M-based positioning and monitoring system," in *Proc. 2011 International Conference on Electronics, Communications and Control (ICECC)*, Sep. 2011, pp. 2624–2627.

[13] T. D. Drysdale and C. J. Vourch, "Planar antenna for transmitting microwave power to small unmanned aerial vehicles," in *Proc. 2016 Loughborough Antennas Propagation Conference (LAPC)*, Nov 2016, pp. 1–4.

[14] M. E. M. Cayamcela, S. R. Angsanto, W. Lim, and A. Caliwag, "An artificially structured step-index metasurface for 10 GHz leaky waveguides and antennas," in *Proc. 2018 IEEE 4th World Forum on Internet of Things (WF-IoT)*, Feb 2018, pp. 568–573.

[15] C. A. Alistarh, P. D. H. Re, T. M. Strober, S. A. Rotenberg, S. K. Podilchak, C. Mateo-Segura, Y. Pailhas, G. Goussetis, Y. Petillot, J. Thompson, and J. Lee, "Millimetre-wave FMCW MIMO radar system development using broadband SIW antennas," in *12th European Conference on Antennas and Propagation (EuCAP 2018)*, April 2018, pp. 1–5.

[16] M. Poveda-Garca, S. K. Podilchak, G. Goussetis, and J. L. Gmez-Tornero, "Millimeter-wave substrate-integrated waveguide based leaky-wave antenna with broadbeam radiation at broadside," in *12th European Conference on Antennas and Propagation (EuCAP 2018)*, April 2018, pp. 1–5.

[17] S. Ramalingam, C. A. Balanis, C. R. Birtcher, S. Pandi, and H. N. Shaman, "Axially modulated cylindrical metasurface leaky-wave antennas," *IEEE Antennas and Wireless Propagation Letters*, vol. 17, no. 1, pp. 130–133, Jan 2018.

[18] A. M. Patel and A. Grbic, "A Printed Leaky-Wave Antenna Based on a Sinusoidally-Modulated Reactance Surface," *IEEE Transactions on Antennas and Propagation*, vol. 59, no. 6, pp. 2087–2096, June 2011.

[19] D. Yang and S. Nam, "Tapered unit cell control of a sinusoidally modulated reactance surface antenna," *IEEE Antennas and Wireless Propagation Letters*, vol. 17, no. 12, pp. 2479–2483, Dec 2018.

[20] H. Oraizi, A. Amini, A. Abdolali, and A. M. Karimimehr, "Design of wideband leaky-wave antenna using sinusoidally modulated impedance surface based on the holography theory," *IEEE Antennas and Wireless Propagation Letters*, vol. 17, no. 10, pp. 1807–1811, Oct 2018.

[21] S. K. Podilchak, L. Matekovits, A. P. Freundorfer, K. Esselle, and Y. M. M. Antar, "Modulated strip-line leaky-wave antenna using a printed grating lens and a surface-wave source," in *Proc. 2010 14th International Symposium on Antenna Technology and Applied Electromagnetics the American Electromagnetics Conference*, July 2010, pp. 1–3.

[22] S. K. Podilchak, L. Matekovits, A. P. Freundorfer, Y. M. M. Antar, and M. Orefice, "Controlled Leaky-Wave Radiation From a Planar Configuration of Width-Modulated Microstrip Lines," *IEEE Transactions on Antennas and Propagation*, vol. 61, no. 10, pp. 4957–4972, Oct 2013.

[23] P. M. Gallo, S. K. Podilchak, and L. Matekovits, "A planar leaky-wave antenna offering well designed leakage on the 2d aperture using printed width modulated microstrip lines," in *Proc. 2017 IEEE International Symposium on Antennas and Propagation USNC/URSI National Radio Science Meeting*, July 2017, pp. 277–278.

[24] N. Montaseri and A. Mallahzadeh, "Broadside radiation in leaky-wave antenna using multiperiodic width-modulated microstrip lines," *IEEE Antennas and Wireless Propagation Letters*, vol. 18, no. 1, pp. 207–211, Jan 2019.

[25] S. F. Mahmoud, Y. M. M. Antar, H. F. Hammad, and A. P. Freundorfer, "Theoretical considerations in the optimization of surface waves on a planar structure," *IEEE Transactions on Antennas and Propagation*, vol. 52, no. 8, pp. 2057–2063, Aug 2004.

[26] J. L. Gomez-Tornero, A. T. Martinez, D. C. Rebenaque, M. Gugliemi, and A. Alvarez-Melcon, "Design of tapered leaky-wave antennas in hybrid waveguide-planar technology for millimeter waveband applications," *IEEE Transactions on Antennas and Propagation*, vol. 53, no. 8, pp. 2563–2577, Aug 2005.

[27] A. J. Martinez-Ros, J. L. Gmez-Tornero, and G. Goussetis, "Flexible pattern synthesis with SIW LWAs," in *Proc. 2012 6th European Conference on Antennas and Propagation (EuCAP)*, March 2012, pp. 229–233.

[28] S. K. Podilchak, A. P. Freundorfer, and Y. M. M. Antar, "Surface-Wave Launchers for Beam Steering and Application to Planar Leaky-Wave Antennas," *IEEE Transactions on Antennas and Propagation*, vol. 57, no. 2, pp. 355–363, Feb 2009.

[29] D. Deslandes, "Design equations for tapered microstrip-to-Substrate Integrated Waveguide transitions," in *Proc. 2010 IEEE MTT-S International Microwave Symposium*, May 2010, pp. 704–707.

[30] E. Miralles, H. Esteban, C. Bachiller, A. Belenguer, and V. E. Boria, "Improvement for the design equations for tapered Microstrip-to-Substrate Integrated Waveguide transitions," in *Proc. 2011 International Conference on Electromagnetics in Advanced Applications*, Sept 2011, pp. 652–655.

[31] N. McLachlan, *Theory and application of Mathieu functions*. Dover Publications, 1964.

[32] J. C. Gutiérrez-Vega, R. Rodrıguez-Dagnino, M. Meneses-Nava, and S. Chávez-Cerda, "Mathieu functions, a visual approach," *American Journal of Physics*, vol. 71, no. 3, pp. 233–242, 2003.

[33] F. Monticone, L. Matekovits, M. Orefice, K. P. Esselle, and G. Vecchi, "Avoiding conductor width discontinuities at the cell borders in width-modulated microstrip line periodic structures," in *Proc. 2010 International Conference on Electromagnetics in Advanced Applications*, Sept 2010, pp. 67–70.

[34] D. R. Jackson, C. Caloz, and T. Itoh, "Leaky-Wave Antennas," *Proceedings of the IEEE*, vol. 100, no. 7, pp. 2194–2206, July 2012.

[35] Rogers corporation. (2010) General information of dielectric constant for rt/duroid 6010.2lm and ro3010 high frequency circuit materials. [Online]. Available: https://www.rogerscorp.com/documents/2379/acs/General-Information-of-Dielectric-Constant-for-RT-duroid-6010-2LM-RO3010-High-Frequency-Circuit-Materials.pdf